COMPARATIVE STUDY ON BIAXIAL LOW-CYCLE FATIGUE BEHAVIOUR OF THREE STRUCTURAL STEELS

Manuel de Freitas, Luis Reis and Bin Li
correspondence: mfreitas@dem.ist.utl.pt

Department of Mechanical Engineering
Instituto Superior Técnico, Av. Rovisco Pais, 1049-001, Portugal

Resumo. Foi realizado um estudo experimental e teórico sobre o comportamento de diferentes materiais, 3 aços estruturais, em fadiga multiaxial, nomeadamente em fadiga oligociclica uniaxial/biaxial. Os ensaios foram realizados utilizando uma máquina servo-hidraulica biaxial (8800 Instron). Os materiais utilizados foram: o aço CK45; o aço AISI 303 e o aço 42CrMo4, temperado e revenido (500ºC). Para avaliar o comportamento em fadiga multiaxial foram considerados dois parâmetros: o encruamento adicional e o factor de não proporcionalidade. Foram consideradas seis trajectorias de carregamento, compostas por tracção/torção cíclicas, uniaxiais e biaxiais. De modo a verificar a influência do encruamento adicional na trajectória de carregamento foram realizadas trajectórias proporcionais e não proporcionais. Os resultados experimentais mostram que os 3 materiais estudados possuem um comportamento, relativamente ao encruamento adicional, muito diferente. Observou-se também que os diferentes materiais estabilizavam em poucos ciclos, a partir do carregamento inicial. Com base no critério da Menor Elipse Circunscritiva é definido o factor de não proporcionalidade. A aplicação dos dois parâmetros anteriormente referidos à metodologia ASME, para a fadiga multiaxial, permite obter uma boa correlação entre os resultados estimados e os experimentais.

Abstract. In this paper the uniaxial/biaxial low-cycle fatigue behaviour of three structural steels (CK45 normalized steel, 42CrMo4 quenched and tempered steel and stainless steel AISI 303) are studied, evaluated and compared. Two fatigue parameters are evaluated for estimating non-proportional fatigue lives: the additional hardening and the factor of non-proportionality. A series of tests of uniaxial/biaxial low-cycle fatigue composed of tension/compression with static or cyclic torsion were carried out on a biaxial servo-hydraulic testing machine Instron 8088. Different loading paths were carried out, including proportional and non-proportional loading paths in order to verify the additional hardening caused by different loading paths. The experiments showed that the three materials studied have very different additional hardening behaviour. Generally, the transient process from the initial loading cycle to stabilized loading cycle has only a few cycles, the stabilized cyclic stress/strain parameters are controlling parameters for fatigue damages. A factor of non-proportionality of the loading paths is evaluated based on the Minimum Circumscribed Ellipse approach. Application of the factor of non-proportionality and the additional hardening coefficient to the ASME methodology for multiaxial loading fatigue, allows a good correlation between the predicted and the experiments results.

1. INTRODUCTION

The study of failures due to fatigue in multiaxial stress states has recently received particular attention. Multiaxial stress states can occur either due to multiaxial loading or to local induced multiaxial stress states (on notches, on contact points, etc.) or due to residual stress states due to machining, etc. In engineering designs, conventional approaches based on uniaxial design may estimate unconservative lives for complicated multiaxial fatigue. For a safe and reliable design of components, it is needed to study the effects of non-proportional loadings on the fatigue damage. Many experiments have shown that the non-proportional multiaxial loading reduce fatigue life significantly, traditional parameters such as the von Mises equivalent strain range may underestimate the fatigue damage for non-proportional multiaxial loading. Due to the problem of unsafety with these approaches, many multiaxial fatigue models have been proposed in recent years [1], based on the critical plane concept, the integral concept and so on.

The objective of this paper is to compare and evaluate fatigue parameters suitable for estimating non-proportional fatigue lives. Since the stabilized cyclic stress/strain fields are essential for fatigue life predictions, local elasto-plastic behaviour of the material are studied firstly. Then, a non-proportional fatigue parameter based on the stabilized cyclic stress/strain is evaluated for correlating the fatigue lives obtained in the tests.

A series of tests of uniaxial/biaxial low-cycle fatigue composed of cyclic tension/compression and cyclic torsion were carried out on a biaxial servo-hydraulic testing machine. Specimens were made of three materials: a CK45 normalized steel, an alloy steel quenched and tempered and a stainless steel. The behaviour of both the uniaxial and torsional stresses during low cycle fatigue is analyzed for different levels of plasticity. Also different loading paths were carried out in order to verify the additional hardening caused by different loading paths.

Depending the loading amplitude and loading level, stress relaxations occur and the stabilized cyclic stress/strain state may be very different from the initial cyclic stress/strain state [2].

A factor of non-proportionality of the loading paths is evaluated based on the Minimum Circumscribed Ellipse approach. Application of the non-proportionality factor and the additional hardening coefficient to the ASME methodology for multiaxial loading, allows a good correlation between the predicted and the experiments results.

2. MATERIAL DATA, SPECIMEN FORM AND TEST PROCEDURE

In order to compare the sensitivity of different materials to proportional and non-proportional loadings, three steels are studied. The materials studied are the CK45 steel normalized, the high strength steel 42CrMo4 and the stainless steel AISI 303. Some of the monotonic mechanical properties of the studied materials are shown in Table 1. The geometry of the specimen used is shown in Fig. 1.

Table 1. Mechanical properties of steels

	CK45	AISI 303	42CrMo4
R_m (MPa)	660	625	1100
$R_{p0.2,monotonic}$ (MPa)	410	330	980
A (%)	23	58	16
E (GPa)	206	178	206
HV	195	174	362

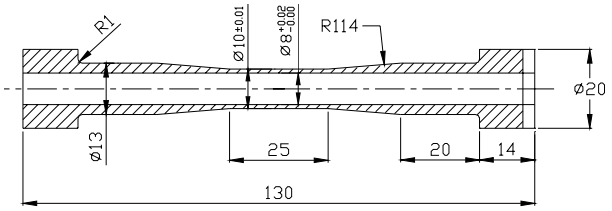

Fig. 1. Specimen geometry for uniaxial/biaxial low cycle fatigue tests

In order to characterize and study the effects of the loading paths on the additional hardening and consequently in the cyclic stress-strain behaviour of the studied materials, a series of low cycle fatigue tests, under proportional and non-proportional paths, as shown in Fig. 2, thick black line, were carried out using a biaxial hydraulic machine (8800 Instron).

All low cycle fatigue tests were fully reversed (R=-1, strain controlled), at a range of frequency between 0.01-0.05 Hz and performed at room temperature. Fig. 3 shows the biaxial extensometer used in the uniaxial/biaxial low cycle fatigue tests.

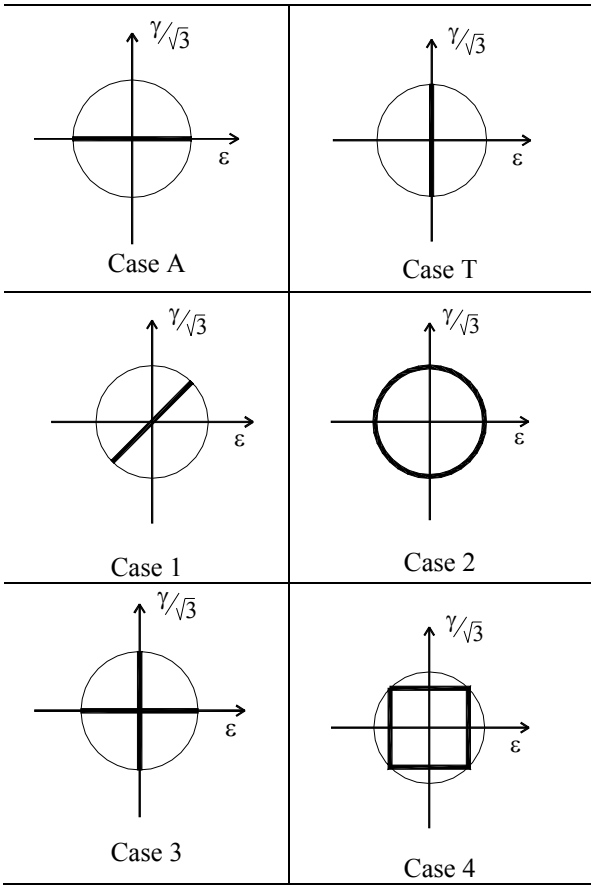

Fig. 2. Multiaxial fatigue loading paths

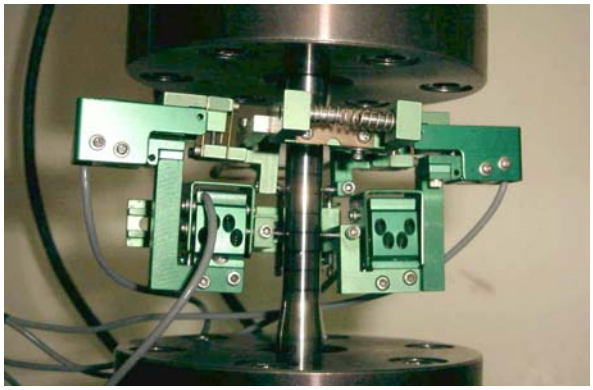

Fig. 3. Biaxial extensometer (model 3550)

3. CYCLIC STRESS-STRAIN RESPONSES

When an elastic-plastic material is subjected to cyclic loading, the stress and strain history will initially go through a transient state which asymptotes to a cyclic state. In this cyclic state, the behaviour of the body can

be characterized by four alternative modes of behaviours [2]: 1- Elastic region. 2-Elastic shakedown. 3-Plastic shakedown. 4- Ratcheting.

Modeling the cyclic behaviour of a material subjected to multiaxial elasto-plastic deformation is essential for predicting the fatigue life of components using multiaxial fatigue criteria.

A convenient method of describing the stable material response is through the cyclic stress-strain curve. Generally, a cyclic stress-strain curve is obtained by connecting the tips of stable hysteresis loops for different strain amplitudes of fully reversed strain-controlled tests. This curve originates the so called ´Masing´curve, Eq. (1):

$$\Delta\varepsilon = \frac{\Delta\sigma}{E} + 2\left(\frac{\Delta\sigma}{2K'}\right)^{1/n'} \quad (1)$$

where K' and n' are the cyclic strength coefficient and cyclic strain hardening exponent, respectively. $\Delta\sigma/2$ and $\Delta\varepsilon/2$ are the stable cycles stress and strain amplitudes, respectively. The cyclic properties obtained from fitting the test results are shown in Table 2, Ref. [3].

Table 2. Cyclic properties of steels

	CK45	**AISI 303**	**42CrMo4**
$R_{p,0.2,cyclic}$ (MPa)	340	310	640
K´(MPa)	1206	2450	1420
n´	0.20	0.35	0.12
σ_f'(MPa)	948	534	1154
b	-0.102	-0.07	-0.061
ε_f'	0.17	0.052	0.18
c	-0.44	-0.292	-0.53

Axial stress σ and shear stress τ were calculated from load and torque measured by a load cell. Axial strain ε and shear strain γ were taken from biaxial extensometer. Equivalent stress $\sigma_{eq.}$ and equivalent plastic strain $\varepsilon^p_{eq.}$ were defined by von Mises equivalence for tension/torsion loading as:

$$\sigma_{eq} = \sqrt{\sigma^2 + 3\tau^2} \quad (2)$$

$$\varepsilon^p_{eq} = \sqrt{\varepsilon^{p2} + \frac{\gamma^{p2}}{3}} \quad (3)$$

and equivalent total strain $\varepsilon_{eq.}$, by analogy [1] as:

$$\varepsilon_{eq} = \sqrt{\varepsilon^2 + \frac{\gamma^2}{3}} \quad (4)$$

4. TYPE OF LOADING AND FACTOR OF NON-PROPORTIONALITY

4.1. Proportional and non-proportional loading

Several definitions of proportional loading are possible. One could be defined as any state of time varying stress where the orientation of the principal stress axes remained fixed with respect to the axes of the component. Non-proportional loading could be defined as any state of time varying stress in which the orientation of the principal axes changes with respect to the axis of the component. From a fatigue viewpoint, a strain history that results in a fixed orientation of the principal axes associated with the alternating components of strain is proportional. The strain history is non-proportional if the principal axes rotate in time, i. e. the corresponding principal directions and/or principal stress ratios vary with time. Only the alternating or cyclic strains are considered because static strains do not influence the direction of reversing shear [1, 4].

4.2. Additional hardening coefficient - α

The additional hardening coefficient α, is a constant of a given material, which is defined as the ratio of equivalent stress under 90º out-of-phase loading and the equivalent stress under proportional loading at high plastic strains in the flat portion of the stress-strain curve, [1].

This coefficient reflects the maximum level of additional hardening that might occur for a given material. The additional hardening coefficient is highly dependent on the microstructure and development of slip systems in a material. In this paper, the additional hardening coefficient is evaluated and compared for the three materials at room temperature.

4.3. Factor of non-proportionality

For non-proportional straining, a rotation of the principal strain axes leads to an additional cyclic strain hardening as compared with that obtained under stable conditions for proportional stressing. In the latter case, dislocations glide on a fixed set of slip planes, whereas for continuously rotating principal axes, many slip systems are activated. Therefore an additional factor must be introduced to represent this extra hardening.

The level of hardening is also dependent on loading history and non-proportionality factors are used to interpolate between the in-phase and out-of-phase

stress-strain curves to obtain a stabilized stress-strain curve for any non-proportional loading history, [1].

To quantify the level of non-proportionality loading path, several ways and some mathematical descriptions have been proposed in the literature. One of them was developed by Kanazawa et al. [5]. These authors proposed a rotation factor, F, to quantify in terms of the amount of slip experienced by critical planes in the specimen, which depends on both phase angle and amplitude. A mathematical description of the non-proportional hardening factor was proposed by Doong, [6]. Another and simple method to evaluate the degree of non-proportionality of the loading paths can be characterized by the MCE (Minimum Circumscribed Ellipse) approach [6]:

$$F_{NP} = \frac{R_b}{R_a} \tag{5}$$

where R_b and R_a are the minor and major radius of the Minimum Circumscribed Ellipse involving the loading path.

5. MULTIAXIAL FATIGUE MODELS FOR CRACK INITIATION LIFE PREDICTION

Many multiaxial fatigue models have been proposed in the last decades [1], some of the recent models require more material parameters and implementation work. Besides, the critical plane concept considers that only the stress/strain states on the critical plane contribute to fatigue damage, which is criticised by some researchers, since the slipping on all the directions may contribute to fatigue damage.

In this paper, the stress-invariant based and the equivalent strain range based multiaxial fatigue models are selected to correlate the experimental results, because these parameters are average measure of the stress/strain states and should be representative damage parameters. To deal with the non-proportional loading effects, appropriate corrections are applied for these parameters as reviewed in following.

5.1. Equivalent Strain Range of ASME Code

The ASME Boiler and Pressure Vessel code Procedure [7] is based on the von Mises hypothesis, but employs the strain difference $\Delta\varepsilon_i$ between time t_1 and t_2:

$$\Delta\varepsilon_{eq} = \frac{1}{(1+\nu)\sqrt{2}}\left\{\left(\Delta\varepsilon_x - \Delta\varepsilon_y\right)^2 + \left(\Delta\varepsilon_y - \Delta\varepsilon_z\right)^2 + \left(\Delta\varepsilon_z - \Delta\varepsilon_x\right)^2 + \frac{3}{2}\left(\Delta\varepsilon_{xy}{}^2 + \Delta\varepsilon_{yz}{}^2 + \Delta\varepsilon_{xz}{}^2\right)\right\}^{1/2} \tag{6}$$

where the equivalent strain range $\Delta\varepsilon_{eq}$ is maximised with respect to time.

Eq. (6) produces a lower equivalent strain range for out-of-phase than the in-phase loading, predicting an increase of the fatigue life, which is in contradiction with experimental results.

5.2. An Improved Model Based on the ASME Code

The ASME Code approach expressed in Eq. (6), define a parameter which has a drawback that is, it produces a lower equivalent strain range for non-proportional than the proportional loading, which underestimates the fatigue damage of non-proportional loading, since many recent experiments have shown that the non-proportional loading reduce the fatigue life significantly than the proportional loading with the same loading amplitude.

In this paper, an improved model based on the ASME code approach is proposed by considering the additional hardening and correcting the strain range parameter for non-proportional loading path:

$$\Delta\varepsilon_{NP} = \left(1 + \alpha F_{NP}\right)\Delta\varepsilon_{eq} \tag{7}$$

where F_{NP} is the non-proportionality factor of the loading path, α is a material constant of additional hardening, $\Delta\varepsilon_{eq}$ is the strain range parameter calculated by Eq.(6), and $\Delta\varepsilon_{NP}$ is the corrected strain range parameter.

Eq. (7) is similar with the approach proposed by Itoh et al. [8], but here the MCE (minimum circumscribed Ellipse) approach developed by M. de Freitas et al [4] previously is applied for evaluating the non-proportionality factor of the loading path.

Then the Manson-Coffin formulation can be used for life predictions:

$$\frac{\Delta\varepsilon_{NP}}{2} = \frac{\sigma'_f - \sigma_m}{E}\left(2N_f\right)^b + \varepsilon'_f\left(2N_f\right)^c \tag{8}$$

where σ_m is the mean stress, E is the young's modulus, σ_f' is the fatigue strength coefficient, ε_f' is the fatigue ductility coefficient, and b and c are fatigue strength and fatigue ductility exponents, respectively.

5.3. MCE Approach for evaluating shear stress amplitude

The idea of the MCE approach is to construct a minimum circumscribed ellipse that can enclose the whole loading path throughout a loading block in the transformed deviatoric stress space. Rather than defining $\sqrt{J_{2,a}} = R_a$ by the minimum circumscribed circle (MCC) approach [9,10], a new definition of $\sqrt{J_{2,a}} = \sqrt{R_a^2 + R_b^2}$ was proposed [4], where R_a and

R_b are the lengths of the major semi-axis and the minor semi-axis of the minimum circumscribed ellipse respectively. The ratio of R_b/R_a represents the non-proportionality of the shear stress path. The important advantage of this new MCE approach is that it can take into account the non-proportional loading effects in an easy way. As shown in Fig. 4, for the non-proportional loading path 1, the shear stress amplitude is defined as $\sqrt{J_{2,a}} = \sqrt{R_a^2 + R_b^2}$. For the proportional loading path 2, it is defined as $\sqrt{J_{2,a}} = R_a$, since R_b is equal to zero (rectilinear loading trace).

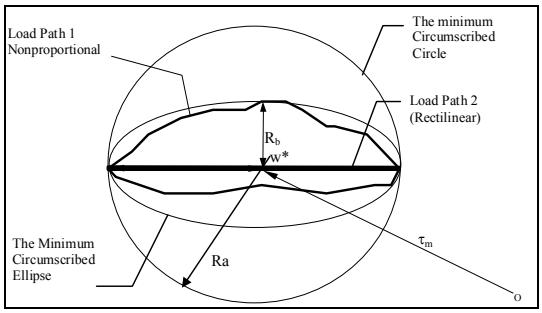

Fig. 4. The MCC and MCE circumscribing to shear stress traces, R_a and R_b are the major and minor radius of MCE, respectively.

6. RESULTS AND DISCUSSIONS

6.1. Cyclic stress-strain behaviour under proportional and non-proportional loading

Proportional cyclic tests were conducted in three directions in the plane (ε , $\gamma/\sqrt{3}$): at 0º, at 45º and at 90º. Non-proportional cyclic tests were conducted with the circle, cross and square paths, respectively (see Fig. 2). Figures 5, 6 and 7 show the cyclic stress-strain responses in terms of equivalent stress amplitude versus equivalent strain amplitude at the stabilized cycles for CK45, AISI 303 and 42CrMo4, respectively.

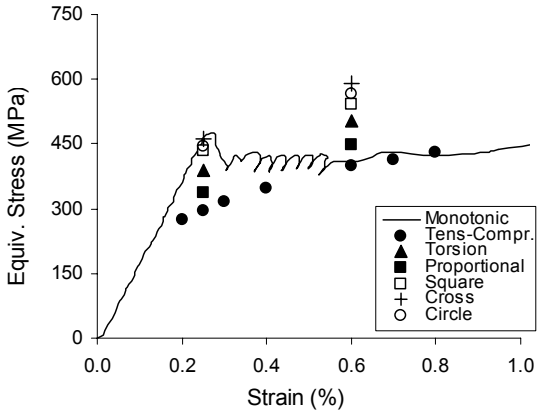

Fig. 5. Cyclic stress-strain responses at the stabilized cycles for six different loading paths of CK45.

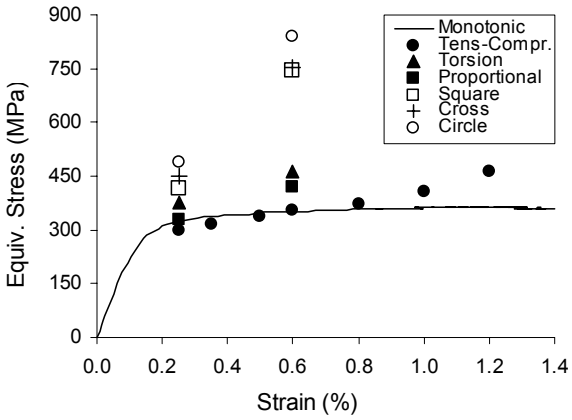

Fig. 6. Cyclic stress-strain responses at the stabilized cycles for six different loading paths of AISI 303.

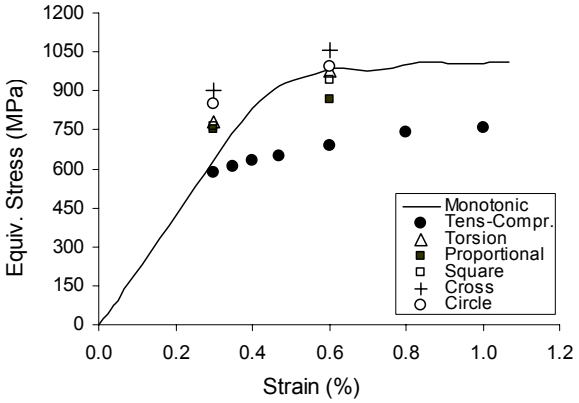

Fig. 7. Cyclic stress-strain responses at the stabilized cycles for six different loading paths of 42CrMo4.

It is shown that, at the same equivalent strain amplitude, the non-proportional loading paths caused much more hardening than the proportional paths.

6.2. Additional hardening coefficient α

For non-proportional straining, a rotation of the principal strain axes leads to an additional cyclic strain hardening over and above that obtained under stable conditions for proportional stressing. In the latter case, dislocations glide on a fixed set of slip planes, whereas for continuously rotating principal axes, many slip systems are activated. Therefore an additional factor must be introduced to represent this extra hardening. In Table 3 the calculated extra hardening values are presented.

Table 3. Values of additional hardening for three materials studied

additional hardening, α	**CK45**	**AISI 303**	**42CrMo4**
	0.3	0.9	0.18

It was observed that the AISI 303 steel is a very sensitive material to non-proportional loading paths

against to the 42CrMo4, which is low sensitive. The circle loading path was the path case that most influences the hardening behaviour for the material studied. As an example, it is possible to observe in Fig.8, for AISI 303 material, loading path case 2 in Fig.2, how stresses increase during the test.

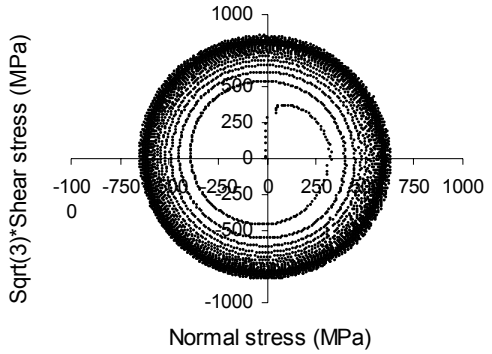

Fig. 8. Non-proportional low cycle fatigue loading, case 2 (AISI 303).

6.3. Comparison of predicted and experimental lives

Only data for the CK45 normalized steel will be presented. The lives of the specimens of CK45 steel subjected to various loading paths were predicted with the improved ASME code approach of Eqs.(7-8). The non-proportionality factor F_{NP} is calculated for each loading path by the MCE approach as described in detail in Ref.[4]. It is shown that the predictions with modified equivalent strain range of the ASME code (Fig. 9) have good accuracy by comparison with experimental results, where the dashed lines represent the error band of factor 2.

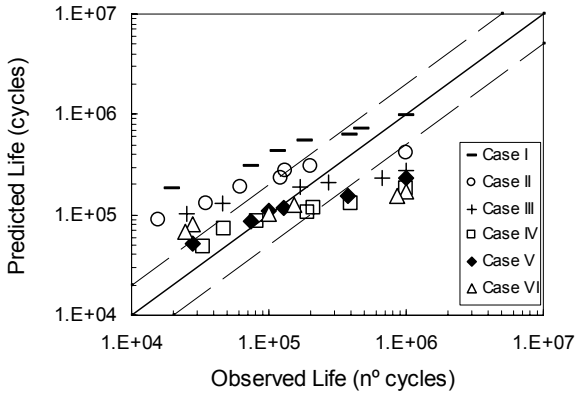

Fig. 8. Experimental versus predicted fatigue life for CK45.

7. CONCLUSIONS

- The local cyclic stress/strain states are influenced by the multiaxial loading paths, due to the interactions between the normal stress and shear stress during cyclic plastic deformation.
- The calculated values of additional hardening coefficient α, have a very good correlation with the values presented in literature.
- The simple and easy of use approaches, such as ASME code and the stress invariant - based approach, can provide good predictions of fatigue life by introducing modifications due to additional hardening and non-proportional effects.

ACKNOWLEDGEMENTS

Financial support from the Fundação para Ciência e Tecnologia (FCT) is acknowledged.

REFERENCES

[1] Socie, D.F. and Marquis, G.B., "Multiaxial Fatigue", Society of Automotive Engineers, Warrendale, PA, (2000).
[2] Ponter, A.R.S. and Carter, K.F., "Shakedown state simulation techniques based on linear elastic solutions", Comput. Methods Appl. Mech. Engrg., 140, 259-279 (1997).
[3] L. Reis, B. Li and M. de Freitas. Biaxial Low-Cycle Fatigue for Proportional and Non-Proportional Loading Paths. "The Fifth International Conference on Low-Cycle Fatigue", pp. 265-270, September, 2003, Berlin, Germany.
[4] M.de Freitas, B. Li and J.L.T. Santos (2000) Multiaxial Fatigue and Deformation: Testing and Prediction, ASTM STP 1387, S. Kaluri and P.J. Bonacuse, Eds., American Society for Testing and Materials, West Conshohocken, PA, pp.139-156.
[5] Kanazawa, K., Miller, K. and Brown, M., Cyclic deformation of 1% Cr-Mo-V steel under out-of-phase loads, Fatigue of Engng Mater Struct, 2, 1979, pp.217-228.
[6] Doong, S. H. and Socie, D. F., Constitutive modelling of metals under nonproportional cyclic loading, Journal of Eng. Mater and Technology, 113, 1991, pp.23-30.
[7] ASME Code Case N-47-23 (1988) Case of ASME Boiler and Pressure Vessel Code, American Society of Mechanical Engineers.
[8] Itoh, T. and Miyazaki, T. (2001) "A damage model for estimating low cycle fatigue lives under non-proportional multiaxial loading", Proceedings of the 6th International Conference on Biaxial/Multiaxial Fatigue & Fracture, Edited by M. de Freitas, Lisbon, June 25-28, pp. 503-510.
[9] I.V. Papadopoulos (1998) Fatigue & Fracture of Engineering Materials & Structures, Vol. 21, pp. 269-285.
[10] Dang-Van, K. (1993) Advances in Multiaxial Fatigue, ASTM STP 1191, D.L. McDowell and R. Ellis, Eds., American Society for Testing and Materials, Philadelphia, pp.120-130.